HHS Public Access

Author manuscript

J Cell Biochem. Author manuscript; available in PMC 2018 May 01.

Published in final edited form as:

J Cell Biochem. 2017 May ; 118(5): 1262–1272. doi:10.1002/jcb.25787.

Histone H4 methyltransferase Suv420h2 maintains fidelity of osteoblast differentiation

Khani Farzaneh[1], **Roman Thaler**[1], **Christopher R. Paradise**[1], **David R. Deyle**[3], **Marianne Kruijthof-de Julio**[4], **Mario Galindo**[5,6], **Jonathan A. Gordon**[7], **Gary S. Stein**[7], **Amel Dudakovic**[1], and **Andre J. van Wijnen**[1,2,*]

[1]Department of Orthopedic Surgery, Mayo Clinic, Rochester, MN, USA [2]Biochemistry and Molecular Biology, Mayo Clinic, Rochester, MN, USA [3]Medical Genetics, Mayo Clinic, Rochester, MN, USA [4]Department of Urology & Department of Clinical Research at University of Bern Bern, Switzerland [5]Millennium Institute on Immunology and Immunotherapy, Institute of Biomedical Sciences, Faculty of Medicine, University of Chile, Santiago, Chile [6]Program of Cellular and Molecular Biology, Institute of Biomedical Sciences, Faculty of Medicine, University of Chile, Santiago, Chile [7]Department of Biochemistry, University of Vermont College of Medicine, 89 Beaumont Avenue, Burlington, Vermont 05405

Abstract

Osteogenic lineage commitment and progression is controlled by multiple signaling pathways (e.g., WNT, BMP, FGF) that converge on bone-related transcription factors. Access of osteogenic transcription factors to chromatin is controlled by epigenetic regulators that generate post-translational modifications of histones ('histone code'), as well as read, edit and/or erase these modifications. Our understanding of the biological role of epigenetic regulators in osteoblast differentiation remains limited. Therefore, we performed next-generation RNA sequencing (RNA-seq) and established which chromatin-related proteins are robustly expressed in mouse bone tissues (e.g., fracture callus, calvarial bone). These studies also revealed that cells with increased osteogenic potential have higher levels of the H4K20 methyl transferase Suv420h2 compared to other methyl transferases (e.g., Suv39h1, Suv39h2, Suv420h1, Ezh1, Ezh2). We find that all six epigenetic regulators are transiently expressed at different stages of osteoblast differentiation in culture, with maximal mRNAs levels of Suv39h1 and Suv39h2 (at day 3) preceding maximal expression of Suv420h1 and Suv420h2 (at day 7) and developmental stages that reflect, respectively, early and later collagen matrix deposition. Loss of function analysis of Suv420h2 by siRNA depletion shows loss of H4K20 methylation and decreased expression of bone biomarkers (e.g., alkaline phosphatase/Alpl) and osteogenic transcription factors (e.g., Sp7/Osterix). Furthermore, Suv420h2 is required for matrix mineralization during osteoblast differentiation. We conclude that Suv420h2 controls the H4K20 methylome of osteoblasts and is critical for normal progression of osteoblastogenesis.

*Corresponding author: Andre J. van Wijnen, Ph.D., Mayo Clinic, 200 First Street SW, Rochester, MN 55905, Phone: 507- 293-2105, Fax: 507-284-5075, vanwijnen.andre@mayo.edu.

Conflict of Interest: Not applicable.

Keywords

Epigenetics; osteoblast; osteocyte; histone; methyl transferase; differentiation; bone; epigenome

Introduction

The epigenetic landscape of chromatin is shaped by regulatory enzymes and scaffolding proteins that are responsible for writing, reading, interpreting, editing and/or erasing post-translational modifications on histone proteins (1). These enzymes may function as pharmacological targets and thus present an enticing opportunity for manipulation of the biological properties of cells during cell growth and differentiation. Recently, we have shown that natural compounds can alter chromatin via active DNA demethylation (2, 3) and that drug-induced inhibition of the H3K27 methyltransferase Ezh2 significantly supports osteoblastic differentiation and bone formation in vitro and in vivo (4, 5). These studies provide proof-of-concept that the activity of epigenetic regulators (EpiRegs) can be leveraged to promote osteogenic lineage progression (6-8), and provide the rationale for investigating the roles of other EpiRegs during osteoblast differentiation.

Transcriptional modulation of select differentiation-related target genes is in principle possible by inhibiting the deposition of active or repressive histone marks. Transcriptionally repressive methyl marks are found on lysine residues at position 9 and 27 on histone H3 and on position 20 on histone H4. The genome-wide presence of these marks in mesenchymal stromal cells and phenotype-committed osteoblasts is controlled by transcription factors that selectively recruit EpiRegs. For example the essential osteoblast-related transcription factor Runx2, nuclear receptors (e.g., vitamin D receptor, Vdr), as well as other transcription factors were shown to modulate several epigenetic mechanisms during osteoblastogenesis (9-12). Furthermore, our group and others recently elucidated how formation of the repressive mark histone 3 lysine 27 trimethylation (H3K27me3) by Ezh2 affects osteoblastic differentiation (4, 5, 13, 14).

Many studies have focused on the three principal methylated lysines of histone H3 (i.e., H3K4, H3K9 and H3K27). Yet, less is known about the role of methylation at histone H4 lysine 20 (i.e., H4K20me1, H4K20me2 and H4K20me3) even though it plays a significant role in cell proliferation (15), and thus is likely to control the transition from cell growth to differentiation. Mono-methylation on Histone H4 lysine 20 methylation (H4K20me1) is associated with transcriptional activation and regulates chromatin condensation and mitotic progression (16). Conversely, tri-methylation on Histone H4 lysine 20 methylation (H4K20me3) is a hallmark of silenced heterochromatic regions, as well as related to repression of transcription and the activity of transposons (17).

Enzymes involved in the methylation of H4K20 are represented by two distinct classes of histone methyltransferases related to the fruit fly ‘suppressor of variegation’ (Suv) proteins, including Suv39 homologues 1 and 2, as well as Suv420 homologues 1 and 2 (respectively, Suv39h1, Suv39h2, Suv420h1 and Suv420h2) (14, 18). SUV proteins utilize the conserved SET domain to methylate lysines on side chains of histone tails. For example, SUV420H2 targets lysine 20 on the histone 4 N-terminal tail (H4K20) (19), while both SUV420H2 and

SUV420H1 recognize the mono-methylated version of H4K20 (H4K20me1) to catalyze the addition of a second methyl group resulting in di-methylated H4K20 (H4K20me2) (20). The substrate specificity of SUV420H2 has been shown to be highly specific for H4K20me1 (21). From genetic and developmental perspectives, global loss of SUV420H1/2 results in perinatal lethality, indicating that these enzymes are principal regulators of normal embryonic patterning, as well as perhaps in self-renewal or lineage-commitment of stem cell populations (22). Indeed, SUV420H2 activity has also been shown to participate in myogenic lineage commitment (23, 24). The functional role of SUV420H2 during myogenic lineage progression may suggest a regulatory role for this protein or other SUV420 homologs during lineage commitment or progression of other mesenchymal cell types, including osteoblastic cells. In this study, we present experimental evidence that SUV39H2 is the most relevant H4K20 methyl transferase during phenotype commitment in osteoblasts and is essential for osteoblast maturation.

Materials and Methods

Cell culture

MC3T3-E1, a clonal pre-osteoblastic cell line derived from newborn mouse calvaria and MLO-A5, a mature osteoblast to pre-osteocyte like cell line established from the long bones of 14-day-old mice (kindly donated by Lynda Bonewald, University of Missouri-Kansas City, USA) were cultured in a humidified atmosphere with 5 % CO_2 at 37 °C and were sub-cultured twice per week using Trypsin (TrypLExpress, Gibco) before achieving confluence. MC3T3-E1 and MLO-A5 cells were cultured in α-minimum essential medium (α-MEM; Gibco) containing 100 units/ml penicillin, and 100 μg/ml streptomycin (Pen-strep, Gibco); for MC3T3-E1 culture media was supplemented with 10 % heat inactivated fetal bovine serum (FBS; Atlanta Biologicals, Flowery Branch, GA) and MLO-A5 cells were cultured on rat-tail derived collagen Type I (Roche) coated dishes (final concentration of 0.15 mg/ml) and culture media was supplemented with 5 % fetal calf serum (FCS, Hyclone) and 5 % calf serum (CS, Hyclone).

Differentiation of MC3T3-E1 cells was induced with 50 μg/ml ascorbic acid (Sigma-Aldrich) and 5 mM β-glycerophosphate (Sigma-Aldrich) in medium containing 10 % FCS. Cells were seeded in culture dishes at a density of 10,000 cells/cm^2. Before cell differentiation was induced, the culture medium was changed.

Suv420h2 siRNA transfections

For *Suv420h2* depletion by siRNA, MC3T3-E1 cells were seeded at 10,000 cells/cm^2 in diverse multiwell plate formats for protein and RNA collection as well as for alkaline phosphatase activity measurements and for extra cellular matrix (ECM) deposition and mineralization assessment by picro sirius red staining and by alizarin red staining, respectively. Six hours after seeding, cells were transfected with scrambled or *Suv420h2* specific siRNA (# L-052050-00, GE Dharmacon) using Lipofectamine RNAiMAX (Invitrogen) as described by the supplier. One day after transfection, medium change was performed and osteoblastic induction was induced as described above. Protein was isolated 3 days after transfection, RNA was isolated 3 days, 6 days and 10 days after transfection,

ECM deposition was analyzed 7 days after transfection, alkaline phosphatase activity was measured 10 days after siRNA transfection and ECM mineralization was analyzed 29 days after siRNA transfection.

Protein isolation and immunoblotting

Whole cell protein extracts were prepared using SDS sample buffer (3 % SDS and 125 mM Tris-HCl, pH= 6.8) and heated at 95°C for 5 min. For immunoblotting analysis, 5 μg of total protein extracts were separated on 11 % SDS poly-acryl amide gels, transferred to polyvinylidene difluoride membranes (Millipore), blocked for 1 hour with 5 % non-fat dry milk in TBST buffer (137mM NaCl, 2.7mM KCl, 19mM Tris, 0.1% Tween). The following primary antibodies were used: rabbit- anti Gapdh (#5174S, Cell Signaling), mouse- anti H4K20me3 (#39672, Active Motif), rabbit- anti-histone H4 (#61200, Active Motif) and rabbit- anti Suv420h2 (#ab91224, Abcam). Washing was performed with TBS buffer containing 0.1 % Tween. Subsequently, binding of the secondary antibody (anti-rabbit IgG/ anti-mouse IgG horseradish peroxidase-coupled) (Santa Cruz) diluted 1:10,000 in 5 % non-fat dry milk in TBST followed by detection with the Amersham ECL Prime Western Blot Detection Reagent (Ge Dharmacon) was carried out as described by the supplier. Chemo-luminescence was measured with an image acquisition system (Chemidoc Touch, Biorad). Measurements are given as means of 3 immuno-blots and representative blots are shown.

Isolation of RNA and reverse-transcriptase quantitative polymerase chain reaction (RT-qPCR)

Total RNA was extracted using the Direct-Zol RNA Mini Prep Kit (Zymo) following the supplier's instructions. cDNA was synthesized from ~0.5 μg RNA using the SuperScript III first strand synthesis system (Invitrogen) as described by the supplier. The resulting cDNAs were subjected to quantitative PCR amplification with a real-time cycler using the QuantiTect SYBR-Green PCR Kit (Qiagen) for the genes *Suv39h1*, *Suv39h2*, *Suv420h1*, *Suv420h2*, *Sp7*, *Bglap2*, *Alpl*, *Runx2*, *Ezh1*, *Ezh2*, *Ccnb2*, *Ibsp*, *Col1a1* and *Gapdh* (for primers, see Table 1). SYBR-Green RT-qPCR was started with an initial denaturation step at 95°C for 15 min and then continued with 45 cycles consisting of 30 sec denaturation at 95°C, 30 sec annealing at 60°C, and 30 sec extension at 72°C in a CFX384 real time system machine (Bio-Rad). All RT-qPCR assays were performed in triplicate and expression was evaluated using the comparative quantification method (25).

Gene expression profiling of mouse cells derived from fracture callus and Ezh2 cKO calvaria

We performed gene expression profiling by next generation RNA sequencing (RNA-seq) of calvaria bone or callus-derived cells in a mouse model for long bone healing derived from fracture callus. Calvarial bone was derived from either wild type mice, or mice in which the Ezh2 gene was conditionally ablated using a Prrx1-Cre driver as previously described (4). Cells derived from the callus were isolated using a lineage-traced method by recombination of a floxed stop allele and activation of downstream red fluorescent protein (tomato) upon activation of a SMACreERT2 reporter (26). This genetic approach permits marking of all cells derived from SMACre expressing mesenchymal stem cells, which are rendered Tomato positive, while Sma-negative cells that include hematopoietic cells remain Tomato-negative.

Callus cell preparations were sorted by flow cytometry to yield Tomato-positive and –negative that were subjected to RNA-seq. Raw read data from all samples were processed using a standard bioinformatic pipeline that has been described in detail previously to obtain values for mRNA levels that are expressed as reads per million mapped reads per kilobasepair.

Relative quantification of ECM deposition

Seven days after *Suv420h2* siRNA transfection, MC3T3-E1 cells were removed using 0.5% sodium deoxycholate. The residual ECM was washed with PBS and stained with picro Sirius red as described before (27, 28). Fluorescence quantification was performed on a Tecan (Maennedorf, Switzerland) multi-well reader.

Alkaline phosphatase activity (ALP)

MC3T3-E1 cells were seeded in 12 multi well culture dishes at a density of 10,000/cm^2 and transfected with Suv420h2 specific or scrambled siRNA as described above. On the next day, the medium was changed and cell differentiation was induced. After ten days, cell number and ALP-activity were analyzed. For determination of cell number (DNA amount employed as surrogate), cell layers were washed with PBS and frozen with 1 mM Tris–HCl buffer (pH 8.0) containing 0.1 mM EDTA. During thawing, Hoechst 33258 dye (Polysciences, Warrington, PA) was added (1 μg/mL) and, after an incubation of 15 min at room temperature, the fluorescence was measured (excitation 360, emission 465 nm). The amount of DNA was estimated using a standard curve prepared from calf thymus DNA (Roche). Thereafter, alkaline phosphatase (ALP) activity was measured with p-nitrophenylphosphate (Sigma) (2.5 mg/mL in 0.1 M diethanolamine buffer [pH 10.5], 150 mM NaCl, 2 mM $MgCl_2$) by incubation of the cell layers for 20 min at room temperature. Absorption was measured in a microplate reader at 405/490 nm. ALP activity per well was estimated using a standard curve prepared from calf intestinal ALP (Roche) and referred to the amount of DNA previously measured.

Alizarin Red staining

For assessment of mineralization, MC3T3-E1 cells were fixed in 4% paraformaldehyde at 29 days after siRNA transfections and 28 days after induction of osteoblastic differentiation. Fixed cells were stained with 40 mM Alizarin Red S (Sigma-Aldrich), pH 4.2, by incubating the cells for 20 min at room temperature. Subsequently, Alizarin Red S dye was extracted using 10% cetylpyridinium chloride in 10 mM sodium phosphate, pH 7.0, for 45 min at room temperature. Alizarin Red S absorbance was measured at 562 nm in a multiplate reader (Tecan) and normalized to total DNA amount which previously measured by Hoechst stain with a multiplate reader (Tecan).

Statistical analysis

Statistical analyses were performed using ANOVA or Student's t test in Prism 4.03 (GraphPad Software). Values of $P \leq 0.05$ were considered significant. Each experiment consisted of at least three biological replicates. For RT-qPCR data, results from technical

triplicates were averaged and the mean value was treated as a single, biological statistical unit. Results are presented as means ± SD.

Results

Transcriptome analysis by next generation sequencing reveals elevated in vivo expression of Suv420h2 in osteoblasts

We performed gene expression profiling using RNA-seq of mouse cells derived from fracture callus and calvaria. RNA-seq values were compared to assess which epigenetic regulators are most specific for mesenchymal cells and bone tissues. Heat-map analysis revealed that there are many epigenetic genes (n=113 out of 345 total) that are selectively expressed at higher levels in mesenchymal cells or tissues with an osteo-chondrogenic biomarker signature (Figure 1A and 1B). Among these genes, we noted that the six methyltransferases *Ezh1*, *Ezh2*, *Suv39h1*, *Suv39h2, Suv420h1* and *Suv420h2* are prominently expressed in callus cells and calvarial tissue (Fig. 1C).

Direct comparison of the six methyltransferases in our study reveals that *Suv420h2* is expressed at the highest mRNA levels compared to *Ezh1*, *Ezh2*, *Suv39h1*, *Suv39h2* and *Suv420h1* (Fig. 2A) in calvarial bone from mice with a conditional Ezh2 null mutation that accelerates osteoblast differentiation and elevates expression of the bone markers *Alp*l and *Ibsp* (Fig. 2B). Furthermore, *Suv420h2* represents the only gene of this set of six that is selectively enriched in mesenchymal cells in the fracture callus at day 6 and that are marked by RFP expression by lineage-tracing (Fig. 2C). These same RFP-positive cells also express very high levels of *Alpl* and *Ibsp* compared to RFP-negative cells in the callus (Fig. 2D). Thus, the RNA-seq data indicate that *Suv420h2* is selectively expressed at higher levels in tissues and cells that robustly express osteoblastic markers. This finding suggests that H4K20 methyl transferase activity may be linked to progression of osteoblast differentiation.

Suv methyltransferases are down-regulated during onset of quiescence and differentiation in MC3T3-E1 osteoblasts and MLO-A5 pre-osteocytes

Having established that *Suv420h2* is strongly expressed in osteogenic cells by RNA-seq, we validated its expression by RT-qPCR in cell culture models for osteoblast and early osteocyte differentiation (Figs. 3 and 4). As expected, the proliferation markers histone H4 (*Hist2h4*) and Cyclin B2 (*Ccnb2*) are down regulated after day 3 in both MC3T3-E1 and MLO-A5 cells (Figs. 3A and 4A). Similarly, *Ezh2*, *Suv39h1* and *Suv39h2* also have peak expression during the early culturing period in MC3T3-E1 cells (Figs. 3B-3C). However, *Ezh1*, *Suv420h1* and *Suv420h2* appear to be expressed at maximal levels at day 7 and their expression gradually fades during progression of osteoblast differentiation over 28 days of MC3T3-E1 cell culture (Figs. 3B-3D). For comparison, expression patterns in MLO-A5 osteocytes tend to be generally similar, albeit more variable and expression changes are less pronounced (Figs. 4B-4D). We note that *Suv420h2* is expressed at lower levels and shows less modulation in its expression compared to *Suv420h1* in MLO-A5 osteocytes (Fig. 4D). Taken together, these data corroborate the in vivo expression data presented in Figure 1 and indicate that *Suv420h2* is actively expressed during osteoblast maturation but is expressed at lower levels after the osteoblast-osteocyte transition.

Suv420h2 controls H4K20 tri-methylation in pre-osteoblastic cells

H4K20 tri-methylation is a hallmark of transcriptional repression and is regulated by Suv420h1 and Suv420h2. Because *Suv420h2* is robustly expressed in osteoblastic cells (see Figs. 1-4), we analyzed the effects of Suv420h2 knock down by siRNA in MC3T3-E1 pre-osteoblasts to understand its functional role in osteoblastogenesis. We observe a clear 2 to 3-fold reduction in Suv420h2 expression at both RNA (Fig. 5A) and protein levels (Fig. 5B-C) at 3 days after siRNA transfection. More importantly, immunoblot analysis shows that depletion of Suv420h2 reduces H4K20me3 levels (Fig. 5D) but not H4K20me1 levels (Fig 5E). These studies support the conclusion that Suv420h2 is rate-limiting for global H4K20me3 levels in MC3T3-E1 cells and thus a major regulator of H4K20me3-directed transcriptional repression during osteoblastogenesis.

Primary osteogenic functions are disrupted after reduction of Suv420h2 expression

Extra cellular matrix (ECM) deposition and its mineralization are among the main activities of differentiating osteoblasts. To elucidate the role of Suv420h2 on ECM maturation during osteoblastogenesis, we analyzed the effect of Suv420h2 depletion by siRNA on ECM deposition around MC3T3-E1 osteoblasts. Collagen fibers were visualized using Picro Sirius Red and staining intensity was determined at day 7 after initiation of osteoblastic differentiation. We observed a modest albeit not significant reduction in ECM deposition in MC3T3-E1 cells treated with *Suv420h2* siRNAs (Fig. 6A). However, alkaline phosphatase activity, an enzyme marker that is deposited in the collagen-rich ECM during osteoblast maturation and ECM mineralization, was significantly decreased at day 10 in cells in which Suv420h2 levels were reduced by siRNA treatment (Fig. 6B). Furthermore, ECM mineralization was significantly reduced by about 25% in MC3T3-E1 cells at day 28 of differentiation (Fig. 6C), even though Suv420h2 expression was only actively suppressed by siRNA during the initial stages of the culture period. The lasting effects of a temporary knock down of Suv420h2 by siRNA indicates that Suv420h2 may affect the molecular memory of MC3T3-E1 cells through epigenetic mechanisms operative at early stages of osteoblastogenesis.

siRNA inhibition of Suv420H2 negatively affects the expression of histone methyltransferases and of primary osteoblastic markers in differentiating MC3T3-E1 cells

Because the long-term effects of Suv420h2 inhibition on osteoblastic differentiation of MC3T3-E1 cells are instigated during the first several days of the culturing period, we analyzed the acute regulatory functions of Suv420h2 by analyzing gene expression of multiple markers and select transcription factors genes in cells in which Suv420h2 expression was reduced by siRNA (see Figure 5). Our analysis focused on day 3 of MC3T3-E1 differentiation (Fig. 7) as a key time-point within a broader time-course up to day 10 (Figs. 7-9). Depletion of Suv420h2 does have small (less than 1.5 fold), although partially significant effects on the expression of other methyltransferases (Fig. 7A). However, cells exhibit 2 to 8 fold a down-regulation of several ECM related osteoblastic genes, including *Sparc*, *Col1a1*, *Alpl* and *Ibsp* (Fig. 7B). We did not detect significant changes in the levels of *Bglap2*, presumably because cells at day 3 in culture are immature and do not have a robust basal level of expression. More importantly, we observed a strong reduction in the

expression of the osteoblastic transcription factor *Sp7* (Osx) at day 3 after *Suv420h2* siRNA transfection, while *Runx2* levels remain relatively constant (Fig. 7C). These results suggest that Suv420h2 alters key osteoblastic markers at early stages of osteoblastic differentiation in cell culture.

Long term effects of transient Suv420h2 inhibition on the expression of primary osteoblastic markers in differentiating MC3T3-E1 cells

Transient depletion of Suv420h2 expression by siRNA for the first three days at early stages of osteoblast differentiation affects late osteoblastic events like ECM mineralization (see Fig. 6C). Therefore, we assessed whether these early reductions in Suv420h2 levels have sustained effects on osteoblastic maturation (Figs. 8 and 9). Interestingly, although MC3T3-E1 cells were treated with *Suv420h2* siRNA for only three days, *Suv420h2* expression remains low throughout the remainder of the time course until day 10 (Fig. 8F). Even though this reduced level of *Suv420h2* has only modest effects on the expression of other epigenetic regulators at day 3 (Figs. 8A-8F; see also Fig. 7A), greater changes in expression of *Ezh2, Suv39h1* and *Suv39h2* are observed at day 6 (Figs. 8B-D). Thus, loss of *Suv420h2* expression may have broad ranging secondary epigenetic effects on gene expression during osteoblast differentiation (Fig. 8F). Furthermore, transient Suv420h2 knock down (Fig. 8F) has primarily transient effects on most osteoblastic markers like *Col1a1*, *Ibsp*, *Alpl* (Figs. 9B-9D) or osteoblastic transcription factors like *Sp7* (Figs. 9E-9F). However, *Suv420h2* siRNA treatment has a delayed effect on the late-stage osteoblast marker *Bglap2* at day 10 (Fig. 9A). We conclude that transient knock down of Suv420h2 has delayed effects on ECM mineralization by altering lysine-methylation related epigenetic mechanisms, and these alterations reduce expression of early osteoblastic markers and delay expression of late osteoblast markers that together control ECM maturation.

Discussion

Epigenetic control of gene expression by histone modifications is a principal regulatory mechanism by which cells control lineage commitment and cell maturation. In this manuscript, we present key evidence for the important role of H4K20 methylation and the related histone methyl transferase Suv420h2 in osteoblastic differentiation. RNA-seq profiling revealed that Suv420h2 expression is elevated in cells and tissues which robustly express osteoblastic markers. Consistent with its functional role in bone cell differentiation, Suv420h2 depletion by siRNA suppresses the maturation potential of MC3T3-E1 pre-osteoblastic cells by reducing Alp activity, ECM mineralization, as well as the expression of osteoblast-related biomarkers (e.g., *Ibsp*, *Col1a1* or *Sp7*). Our finding that Suv420h2 is a positive regulator of osteoblast differentiation complements our previous studies that established the importance of other epigenetic regulators, including the H3K27 methyl transferase EZH2 (4, 5), DNA hydroxymethylases TET1 and TET2 (2, 3), DNA methyl-transferases (29, 30) and histone deacetylases (31). Interestingly, each of these epigenetic regulators are enzymes whose activity can be modulated by natural or synthetic inhibitors that strongly affect the differentiation potential of osteoblasts (2, 3, 6, 12). Taken together, our studies corroborate general concepts in the field that the epigenome of osteoblasts is

critical for responses to osteogenic signaling pathways and ligands (e.g., WNT, BMP2, Vitamin D3) (14, 32-35).

We observed that short term depletion of Suv420h2 expression by siRNA treatment decreases H4K20 methylation, and immediately disrupts the natural temporal expression of early osteoblast-specific genes including *Alpl*, *Sp7*, *Col1a1*, *Ibsp* and *Sparc*, as well as that of the late osteoblastic marker *Bglap2*. These disruptions in the temporal sequence of bone specific gene expression clarify the observed inhibition of ECM mineralization upon disruption of Suv420h2-mediated H4K20 methylation. Importantly, we observed these biological effects when osteoblastic cells treated with siRNA for 1 day prior to the induction of osteoblast differentiation during a time course that lasts up to 28 days. Thus, Suv420h2 might play a role in the epigenetic programming of specific osteoblastic pathways at early differentiation stages. The attenuation in ECM mineralization indicates that epigenetic priming of osteoblastic cells at early osteoblastic differentiation stages has relatively long term consequences.

The biological importance and molecular significance of H4K20 methylation by Suv420h2 has not yet been fully resolved. For example, mono-methylation of H4K20 is related to transcriptional activation (16). However, H4K20me2 and H4K20me3 histone marks have been reported to be important for silencing gene expression through formation of heterochromatic regions (17). Our studies which show that Suv420h2 is a key epigenetic regulator in osteoblasts will provide a strong impetus for future studies aimed at defining the specific role of H4K20 mono-, di- and tri-methylation during osteoblast differentiation, skeletal development and bone homeostasis in vivo.

Acknowledgments

We thank our colleagues at Mayo Clinic, and especially Jennifer Westendorf for support and stimulating discussions. We also thank Dr. Lynda Bonewald (University of Missouri-Kansas City, Kansas, MI, USA) for generously providing cell lines. We also appreciate the assistance of Ivo Kalajzic and for providing sorted lineage-traced cells derived from a mouse fracture healing model.

Funding: This work was supported by the National Institute of Arthritis and Musculoskeletal and Skin Diseases [R01 AR049069 to AJVW; F32 AR066508 to AD] and a fellowship grant from the Center of Regenerative Medicine at Mayo Clinic (to RT) as well as by the Fondo Nacional de Desarrollo Científico y Tecnológico (FONDECYT) grant number: 1130931 (to MG), and Iniciativa Científica Milenio. Ministerio de Economía, Fomento y Turismo grant number P09/016-F (to MG). We also appreciate the generous philanthropic support of William H. and Karen J. Eby, and the charitable foundation in their names.

References

1. Ruthenburg AJ, Li H, Patel DJ, Allis CD. Multivalent engagement of chromatin modifications by linked binding modules. Nat Rev Mol Cell Biol. 2007; 8(12):983–994. [PubMed: 18037899]
2. Thaler R, et al. Anabolic and Antiresorptive Modulation of Bone Homeostasis by the Epigenetic Modulator Sulforaphane, a Naturally Occurring Isothiocyanate. J Biol Chem. 2016; 291(13):6754–6771. [PubMed: 26757819]
3. Thaler R, Spitzer S, Karlic H, Klaushofer K, Varga F. DMSO is a strong inducer of DNA hydroxymethylation in pre-osteoblastic MC3T3-E1 cells. Epigenetics. 2012; 7(6):635–651. [PubMed: 22507896]
4. Dudakovic A, et al. Epigenetic Control of Skeletal Development by the Histone Methyltransferase Ezh2. J Biol Chem. 2015; 290(46):27604–27617. [PubMed: 26424790]

5. Dudakovic A, et al. Enhancer of Zeste Homolog 2 Inhibition Stimulates Bone Formation and Mitigates Bone Loss Due to Ovariectomy in Skeletally Mature Mice. J Biol Chem. 2016
6. Fu B, et al. Epigenetic regulation of BMP2 by 1,25-dihydroxyvitamin D3 through DNA methylation and histone modification. PLoS One. 2013; 8(4):e61423. [PubMed: 23620751]
7. Hemming S, et al. EZH2 and KDM6A act as an epigenetic switch to regulate mesenchymal stem cell lineage specification. Stem Cells. 2014; 32(3):802–815. [PubMed: 24123378]
8. Sabbattini P, et al. An H3K9/S10 methyl-phospho switch modulates Polycomb and Pol II binding at repressed genes during differentiation. Mol Biol Cell. 2014; 25(6):904–915. [PubMed: 24430871]
9. Li Y, Ge C, Franceschi RT. MAP Kinase-Dependent RUNX2 Phosphorylation Is Necessary for Epigenetic Modification of Chromatin During Osteoblast Differentiation. J Cell Physiol. 2016
10. Meyer MB, Benkusky NA, Lee CH, Pike JW. Genomic determinants of gene regulation by 1,25-dihydroxyvitamin D3 during osteoblast-lineage cell differentiation. J Biol Chem. 2014; 289(28): 19539–19554. [PubMed: 24891508]
11. Seth-Vollenweider T, Joshi S, Dhawan P, Sif S, Christakos S. Novel mechanism of negative regulation of 1,25-dihydroxyvitamin D3-induced 25-hydroxyvitamin D3 24-hydroxylase (Cyp24a1) Transcription: epigenetic modification involving cross-talk between protein-arginine methyltransferase 5 and the SWI/SNF complex. J Biol Chem. 2014; 289(49):33958–33970. [PubMed: 25324546]
12. St John HC, et al. The osteoblast to osteocyte transition: epigenetic changes and response to the vitamin D3 hormone. Mol Endocrinol. 2014; 28(7):1150–1165. [PubMed: 24877565]
13. Aguilar R, et al. Polycomb PRC2 complex mediates epigenetic silencing of a critical osteogenic master regulator in the hippocampus. Biochim Biophys Acta. 2016; 1859(8):1043–1055. [PubMed: 27216774]
14. Gordon JA, Stein JL, Westendorf JJ, van Wijnen AJ. Chromatin modifiers and histone modifications in bone formation, regeneration, and therapeutic intervention for bone-related disease. Bone. 2015; 81:739–745. [PubMed: 25836763]
15. Jorgensen S, Schotta G, Sorensen CS. Histone H4 lysine 20 methylation: key player in epigenetic regulation of genomic integrity. Nucleic Acids Res. 2013; 41(5):2797–2806. [PubMed: 23345616]
16. Beck DB, Oda H, Shen SS, Reinberg D. PR-Set7 and H4K20me1: at the crossroads of genome integrity, cell cycle, chromosome condensation, and transcription. Genes Dev. 2012; 26(4):325–337. [PubMed: 22345514]
17. Schotta G, et al. A silencing pathway to induce H3-K9 and H4-K20 trimethylation at constitutive heterochromatin. Genes Dev. 2004; 18(11):1251–1262. [PubMed: 15145825]
18. Bradley EW, Carpio LR, van Wijnen AJ, McGee-Lawrence ME, Westendorf JJ. Histone Deacetylases in Bone Development and Skeletal Disorders. Physiol Rev. 2015; 95(4):1359–1381. [PubMed: 26378079]
19. Wu H, et al. Crystal structures of the human histone H4K20 methyltransferases SUV420H1 and SUV420H2. FEBS Lett. 2013; 587(23):3859–3868. [PubMed: 24396869]
20. Southall SM, Cronin NB, Wilson JR. A novel route to product specificity in the Suv4-20 family of histone H4K20 methyltransferases. Nucleic Acids Res. 2014; 42(1):661–671. [PubMed: 24049080]
21. Yang H, et al. Preferential dimethylation of histone H4 lysine 20 by Suv4-20. J Biol Chem. 2008; 283(18):12085–12092. [PubMed: 18296440]
22. Schotta G, et al. A chromatin-wide transition to H4K20 monomethylation impairs genome integrity and programmed DNA rearrangements in the mouse. Genes Dev. 2008; 22(15):2048–2061. [PubMed: 18676810]
23. Tsang LW, Hu N, Underhill DA. Comparative analyses of SUV420H1 isoforms and SUV420H2 reveal differences in their cellular localization and effects on myogenic differentiation. PLoS One. 2010; 5(12):e14447. [PubMed: 21206904]
24. Neguembor MV, et al. FSHD muscular dystrophy region gene 1 binds Suv4-20h1 histone methyltransferase and impairs myogenesis. J Mol Cell Biol. 2013; 5(5):294–307. [PubMed: 23720823]
25. Pfaffl MW. A new mathematical model for relative quantification in real-time RT-PCR. Nucleic acids research. 2001; 29(9):e45. [PubMed: 11328886]

26. Matthews BG, et al. Analysis of alphaSMA-labeled progenitor cell commitment identifies notch signaling as an important pathway in fracture healing. J Bone Miner Res. 2014; 29(5):1283–1294. [PubMed: 24190076]

27. Thaler R, et al. Homocysteine induces serum amyloid A3 in osteoblasts via unlocking RGD-motifs in collagen. FASEB J. 2013; 27(2):446–463. [PubMed: 23085993]

28. Thaler R, et al. Differential effects of homocysteine and beta aminopropionitrile on preosteoblastic MC3T3-E1 cells. Bone. 2010; 46(3):703–709. [PubMed: 19895920]

29. Thaler R, et al. Homocysteine suppresses the expression of the collagen cross-linker lysyl oxidase involving IL-6, Fli1, and epigenetic DNA methylation. J Biol Chem. 2011; 286(7):5578–5588. [PubMed: 21148317]

30. Thaler R, Karlic H, Spitzer S, Klaushofer K, Varga F. Extra-cellular matrix suppresses expression of the apoptosis mediator Fas by epigenetic DNA methylation. Apoptosis. 2010; 15(6):728–737. [PubMed: 20428952]

31. Dudakovic A, et al. Histone deacetylase inhibition promotes osteoblast maturation by altering the histone H4 epigenome and reduces Akt phosphorylation. J Biol Chem. 2013; 288(40):28783–28791. [PubMed: 23940046]

32. Meyer MB, Benkusky NA, Sen B, Rubin J, Pike JW. Epigenetic Plasticity Drives Adipogenic and Osteogenic Differentiation of Marrow-derived Mesenchymal Stem Cells. J Biol Chem. 2016; 291(34):17829–17847. [PubMed: 27402842]

33. Lee SM, Meyer MB, Benkusky NA, O'Brien CA, Pike JW. Mechanisms of Enhancer-mediated Hormonal Control of Vitamin D Receptor Gene Expression in Target Cells. J Biol Chem. 2015; 290(51):30573–30586. [PubMed: 26504088]

34. Stein GS, et al. Architectural genetic and epigenetic control of regulatory networks: compartmentalizing machinery for transcription and chromatin remodeling in nuclear microenvironments. Crit Rev Eukaryot Gene Expr. 2010; 20(2):149–155. [PubMed: 21133844]

35. Wu H, et al. Genomic occupancy of Runx2 with global expression profiling identifies a novel dimension to control of osteoblastogenesis. Genome Biol. 2014; 15(3):R52. [PubMed: 24655370]

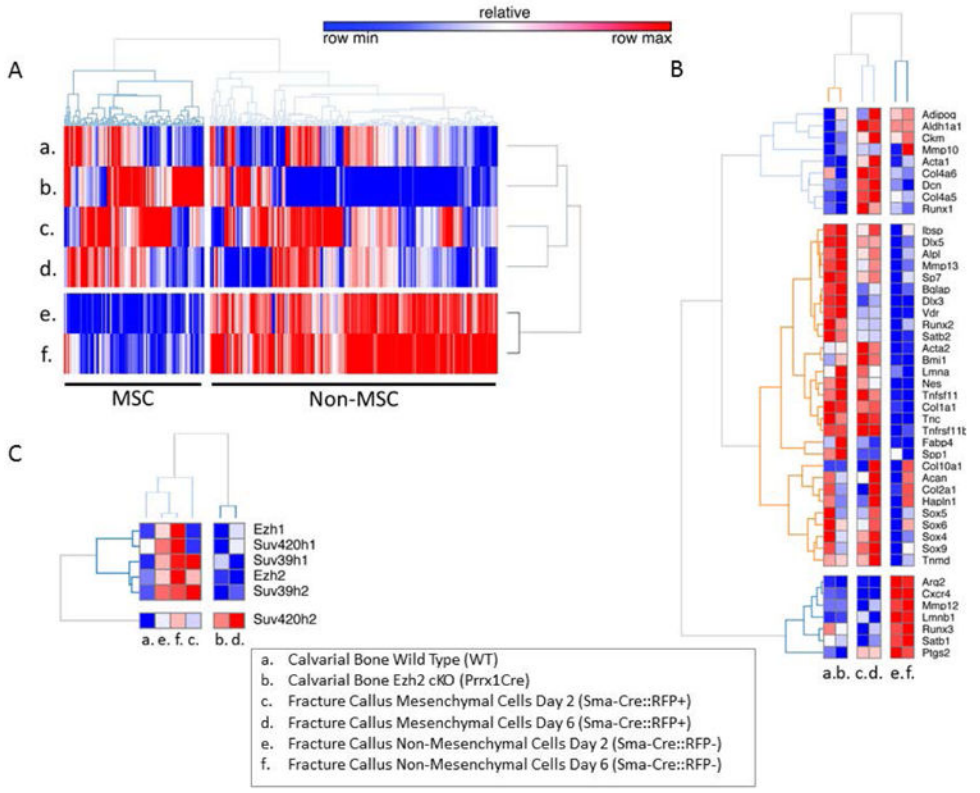

Figure 1. Heat-map analysis of different bone tissues

Gene expression patterns for epigenetic regulators (A) osteoblastic biomarkers (B) and histone methyltransferases (C) in wild type (WT) calvarial bone, Prxx1-Cre driven conditional knock out of Ezh2 in calvarial bone, as well as mesenchymal cells (Sma-Cre driven, RFP-pos) and non-mesenchymal cells (Sma-Cre driven, RFP-neg) in fracture callus at day 2 and day 6 as measured by RNA-seq analysis with values expressed as Reads Per Kilobase of transcript per Million mapped reads (RPKM). Low and high levels of gene expression are shown in, respectively, blue (row min) and red (row max). The sample codes are provided in the insert.

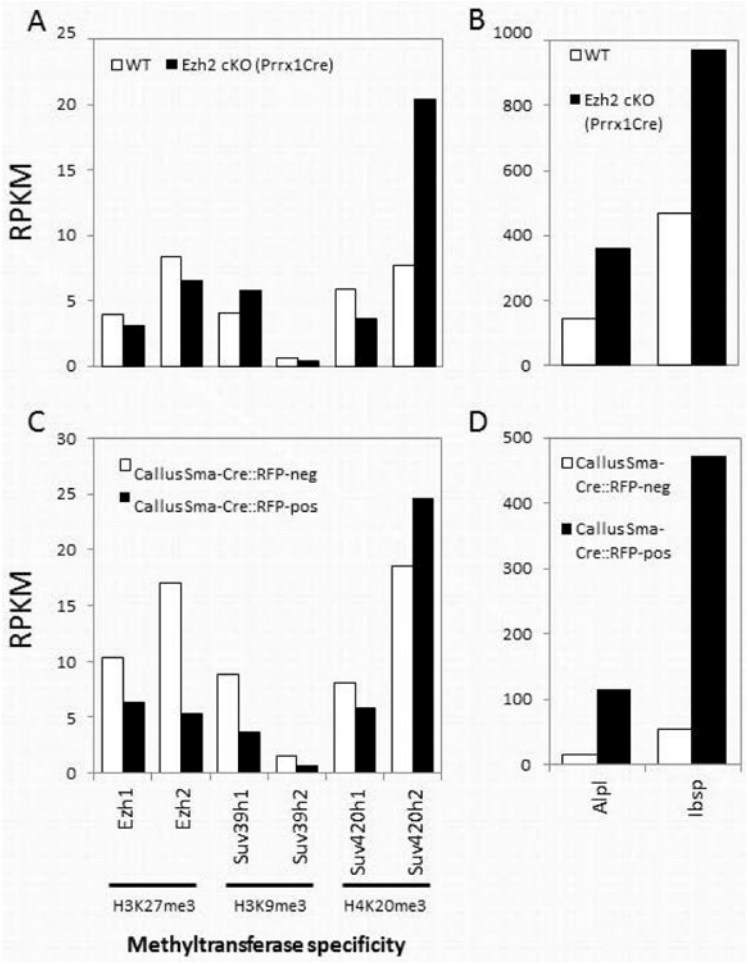

Figure 2. RNA-seq analysis of selected histone methyltransferases in different bone tissues

Levels of mRNAs for selected histone methyltransferases (A and C) and of osteoblastic markers (B and D) in wild type (WT, white bars) versus Ezh2 negative (Ezh2 cKO – Prrx1Cre, black bars) calvarial bone (A and B) as well as in mesenchymal cells (Callus Sma-Cre::RFP-pos, black bars) versus non mesenchymal cells (Callus Sma-Cre::RFP-neg, white bars) from fracture callus at day 6 (C and D) as measured by RNA-seq analysis with values expressed as RPKM.

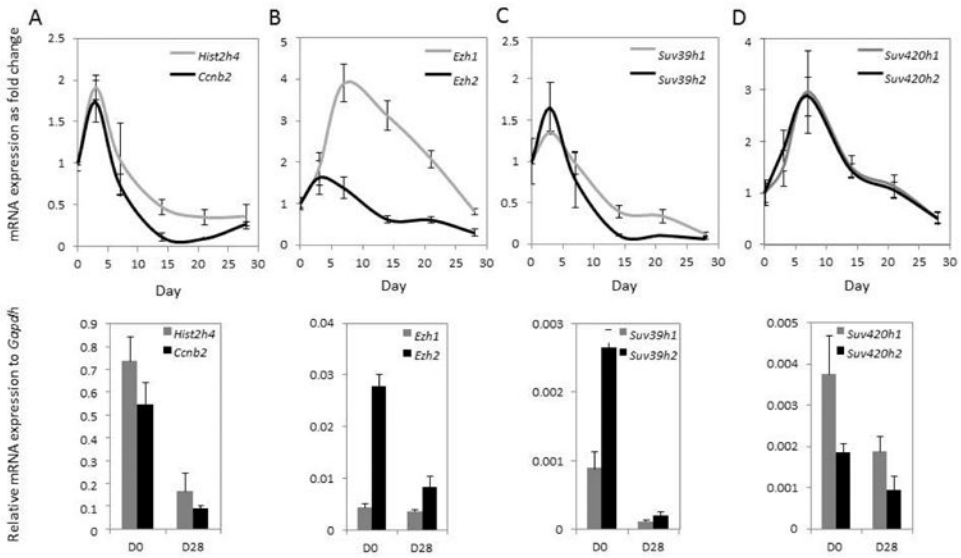

Figure 3. Differential expression of epigenetic regulators during osteogenic commitment of MC3T3-E1 cells

mRNA expression levels of cell cycle markers (A) and selected histone methyltransferases (B-D) during osteoblastic differentiation of MC3T3-E1 cells as measured by RT-qPCR. *Gapdh* was used as reference gene for RT-qPCR analysis; in the upper panel each gene is set to 1 at day 0 and all other days are referred as fold change relative to day 0 (D0). Day 0 represents the beginning of differentiation in subconfluent cells. The lower panel depicts the relative expression of each gene relative to *Gapdh* at the beginning of differentiation at day 0 and at the end of differentiation at day 28 (D28). Values are represented as mean ± SD; for all experiments $n = 3$.

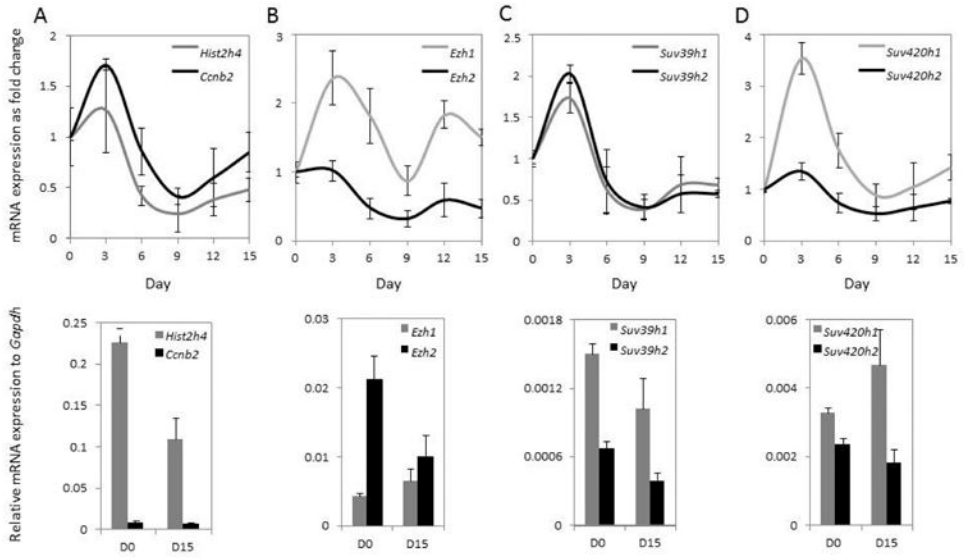

Figure 4. Expression of epigenetic regulators during osteoblastic differentiation of MLO-A5 cells

mRNA expression levels of cell cycle markers (A) and selected histone methyltransferases (B-D) during late osteoblast to early osteocyte differentiation of MLO-A5 cells as measured by RT-qPCR. *Gapdh* was used as reference gene for RT-qPCR analysis; in the upper panel each gene is set to 1 at day 0 and all other days are referred as fold change to day 0. The lower panel depicts the relative expression of each gene to *Gapdh* at the beginning of differentiation at day 0 (D0) and at the end of differentiation at day 15 (D15). Values are represented as mean ± SD; for all experiments $n = 3$.

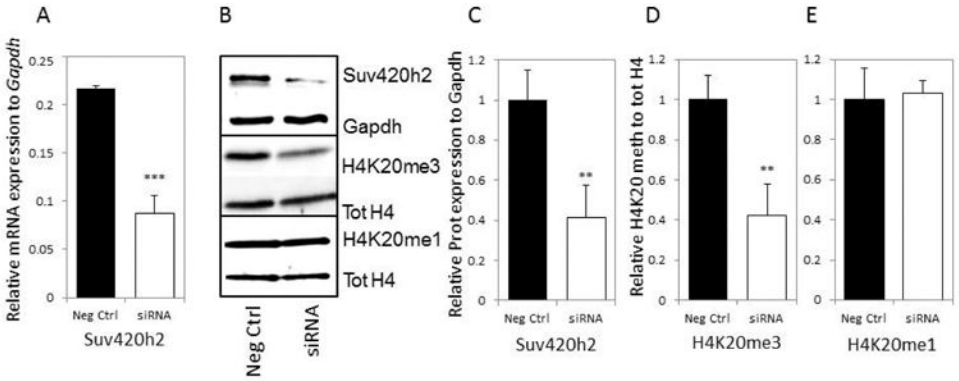

Figure 5. Effects of Suv420h2 knock down after 3 days in MC3T3-E1 cells

Suv420h2 is significantly inhibited at the mRNA expression level by knock-down using siRNA (A). This effect is also observed at the protein level (B-C) and is accompanied by a significant reduction of H4K20me3 levels (D). No alterations were measured for H4K20me1 levels after Suv420h2 knock down (E). Values for mRNA expression were measured by RT-qPCR and *Gapdh* was used as the reference gene in A; representative western blot pictures are shown in B. Values are represented as mean ± SD; for all experiments $n = 3$. ** $P \leq 0.01$.

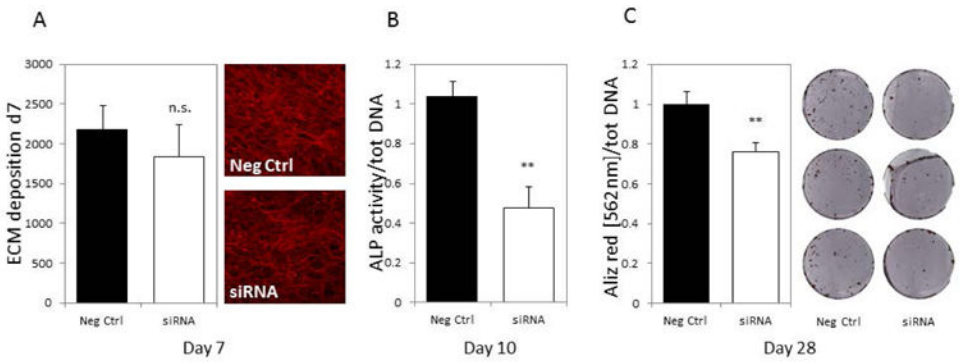

Figure 6. Effects of Suv420h2 knock down by siRNA on primary osteoblastic markers in differentiating MC3T3-E1 cells

Transient Suv420h2 knock down slightly, although not significantly (n.s.) affects ECM deposition at day7 (A). However, at day 10 ALP activity (B) and at day 28 ECM mineralization (C) are significantly reduced in MC3T3-E1 cells initially treated with Suv420h2 siRNA. ECM deposition is measured by Picro Sirius red stain in A, representative ECM images are shown in A; ECM mineralization is determined by Alizarin red staining, representative ECM mineralized images are shown in C. Values are represented as mean ± SD; for all experiments $n = 3$. ** $P \leq 0.01$.

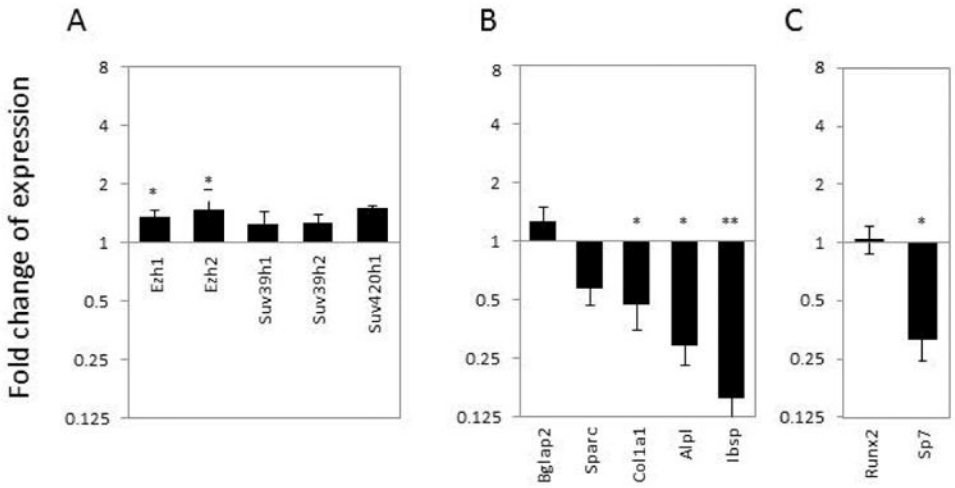

Figure 7. Acute effects of Suv420h2 silencing by siRNA in MC3T3-E1 cells

Fold change in gene expression for selected histone methyltransferases (A), osteoblastic ECM markers (B) and primary osteoblastic transcription factors (C) in Suv420h2 siRNA treated cells at day 3 of differentiation as measured by RT-qPCR. Fold change was calculated relative to scrambled siRNA treated cells at 3 days of differentiation, *Gapdh* was used as housekeeping gene. Values are represented as mean ± SD; for all experiments $n = 3$. * $P \leq 0.05$, ** $P \leq 0.01$.

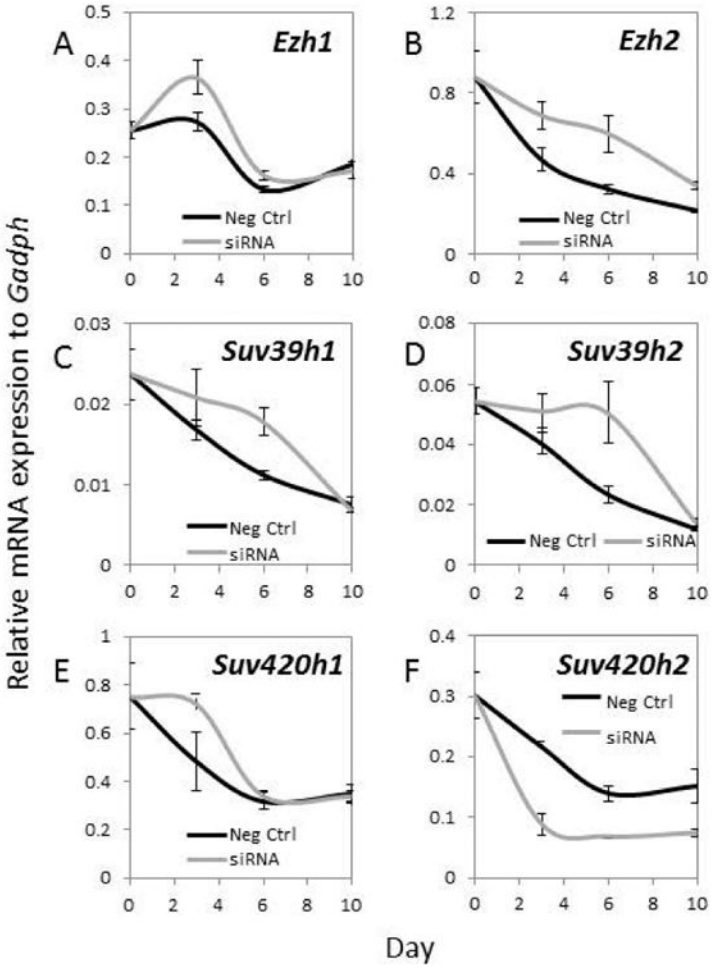

Figure 8. Time related mRNA expression pattern of selected histone methyltransferases after Suv420h2 silencing by siRNA in MC3T3-E1 cells

Gene expression values were measured by RT-qPCR and normalized relative to *Gapdh*. Values are represented as mean ± SD; for all experiments $n = 3$.

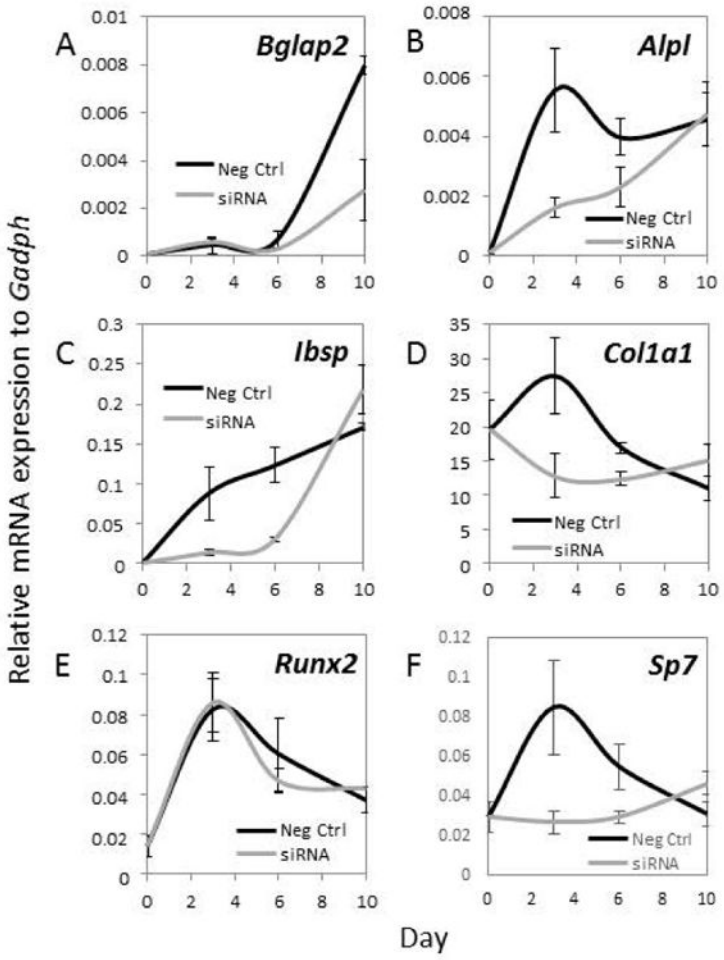

Figure 9. Time related mRNA expression pattern of osteoblastic markers and transcription factors after Suv420h2 silencing by siRNA in MC3T3-E1cells

Gene expression values were measured by RT-qPCR and normalized relative to *Gapdh*. Values are represented as mean ± SD; for all experiments $n = 3$.

Table 1

Sequences of RT-qPCR expression primers

	Fwd primer	Rev primer
Alp1	CCAGAAAGACACCTTGACTGTGG	TCTTGTCCGTGTCGCTCACCAT
Bgiap2	GCAATAAGGTAGTGAACAGACTCC	CCATAGATGCGTTTGTAGGCGG
Ccnb2	GCACTACCATCCTTCTCAGGTG	TGTGCTGCATGACTTCCAGGAC
Colla1	CCTCAGGGTATTGCTGGACAAC	CAGAAGGACCTTGTTTGCCAGG
Ezh1	TGCGTCTCAGGATGGAGGA	TTGCTATATCCATTTTCCTCATGGA
Ezh2	CCTTCCATGCAACACCCAAC	CCTTAGCTCCCTCCAGATGC
Hist2h4	AAGGTTCTCCGCGACAACATCC	GTCGCGGATCACATTCTCAAGG
Ibsp	GAATGGCCTGTGCTTTCTCG	CCGGTACTTAAAGACCCCGTT
Runx2	CCTGAACTCTGCACCAAGTCCT	TCATCTGGCTCAGATAGGAGGG
Sp7	GGCTTTTCTGCGGCAAGAGGTT	CGCTGATGTTTGCTCAAGTGGTC
Sparc	CCCCTCAGCAGACTGAAGTT	ACAGGTACCCCTGTCTCCTC
Suv39h1	AGGAGCGGCCAATCGAC	CAGCACACACTGCAACCTTT
Suv39h2	GCCTTATTCAAGGCCTGGTG	GTCACACAAGTACTCCACCTCA
Suv420h1	CGGCTGCTTCCAACTCTACC	AGTGATTCCGCAGTCTGATCT
Suv420h2	GCAGAGCTGCGTGAAGAGG	ACAGGCAGTATTCCCATCTGA